



LAWRENCE
LIVERMORE
NATIONAL
LABORATORY

Microwave Interrogation of an Air Plasma Plume as a Model System for Hot Spots in Explosives

R. J. Kane, J. W. Tringe, G. L. Klunder, E. V. Baluyot, J. M. Densmore, M. C. Converse

August 3, 2015

19th Biennial Conference on Shock Compression of
Condensed Matter
Tampa, FL, United States
June 14, 2015 through June 19, 2015

Disclaimer

This document was prepared as an account of work sponsored by an agency of the United States government. Neither the United States government nor Lawrence Livermore National Security, LLC, nor any of their employees makes any warranty, expressed or implied, or assumes any legal liability or responsibility for the accuracy, completeness, or usefulness of any information, apparatus, product, or process disclosed, or represents that its use would not infringe privately owned rights. Reference herein to any specific commercial product, process, or service by trade name, trademark, manufacturer, or otherwise does not necessarily constitute or imply its endorsement, recommendation, or favoring by the United States government or Lawrence Livermore National Security, LLC. The views and opinions of authors expressed herein do not necessarily state or reflect those of the United States government or Lawrence Livermore National Security, LLC, and shall not be used for advertising or product endorsement purposes.

Microwave Interrogation of an Air Plasma Plume as a Model System for Hot Spots in Explosives

Ronald J. Kane^{a)} Joseph W. Tringe, Greg L. Klunder, Emer V. Baluyot,
John M. Densmore and Mark C. Converse

*Energetic Materials Center
Lawrence Livermore National Laboratory
Livermore, CA 94550*

^{a)}kane2@llnl.gov

Abstract. The evolution of hot spots within explosives is critical to understand for predicting how detonation waves form and propagate. However, it is challenging to observe hot spots directly because they are small (~micron diameter), form quickly (much less than a microsecond), and many explosives of interest are optically opaque. Microwaves are well-suited to characterize hot spots because they readily penetrate most explosives. They also have sufficient temporal and spatial resolution to measure the coalescence of an ensemble of hot spots inside explosives. Here we employ 94 GHz microwaves to characterize the evolution of individual plasma plumes formed by laser ionization of air. We use interferometry to obtain velocity records as a function of plume position and orientation. Although the plasma plumes are larger than individual hot spots in explosives, they expand rapidly and predictably, and their structure can be optically imaged. They are therefore useful model systems to establish the spatial and temporal limits of microwave interferometry (MI) for understanding more complex hot spot behavior in solid explosives.

INTRODUCTION

Microwave interferometry has been used for decades to measure the velocity of detonation fronts in explosives.¹⁻⁹ It is effective because the detonation front itself is highly reflective to microwaves, while the majority of common explosives do not readily absorb electromagnetic radiation at microwave frequencies.¹⁰ Relevant to work reported here, one important study measured the reflectivity of explosive particles mixed with known volume fractions of microwave-reflective metal particles to calibrate the effective hot spot density in a shock-initiated detonation wave.⁶ Although the metal particles were much smaller than the interrogating wavelength, as an ensemble in a waveguide the metal particles present a partially-reflecting surface. The higher the density of metal particles, the larger the fraction of reflected microwave energy.

In experiments unrelated to explosives, pulses of focused laser light have been shown to locally ionize air, producing a plasma domain that expands and collapses over a period of milliseconds, when pulse durations are ps to ns. The plasma plume has been imaged over time using fast cameras, such that the luminous plasma is clearly visible in the center of an expanding shock wave in air.¹¹⁻¹³ Typically the plasma expansion velocity in the direction parallel to the laser beam propagation direction is much faster than the expansion velocity in the radial direction perpendicular to the beam. This is because air is heated in all along the beam at rate which is inversely proportional to the beam's cross sectional area, as the beam focused to a few microns at its narrowest point. Outside the beam, air remains at ambient temperature. For laser power 180 mJ and duration 20 ns, the plasma plume diameter is about 4 mm at 1 μ s after initiation.¹¹ As this dimension is comparable to the wavelength of the 94 GHz microwaves used in this study, the plume reflects the microwave energy.

METHODS

Light from a Q-switched neodymium-doped yttrium aluminum garnet (Nd:YAG) laser was frequency doubled to produce 532 nm pulses, 10 ps long, at energies between 11 and 40 mJ. Light was focused with a lens immediately in front of a rectangular WR-10 waveguide, such that an ionized plume was produced 3-9 mm from front the waveguide edge. In some experiments the laser propagation direction was parallel to the plane of the rectangular waveguide termination. In other experiments, the laser propagation direction was perpendicular to this plane, aligned with the axis of the waveguide.

94 GHz signals from a microwave interferometer (Millitech) were used to interrogate the laser plume at a power of ~ 1 W. The 94 GHz RF energy reference and scattered signals were mixed down to ~ 1.5 GHz, filtered and digitized by an oscilloscope. Triggering was achieved with a photodetector in the laser beam path. A fast camera imaged the plume at rates of about 100,000 frames per second. The experimental configuration is shown in Figure 1. Mirrors were used to guide the laser light to an imaging lens, and to orient the laser relative to the waveguide.

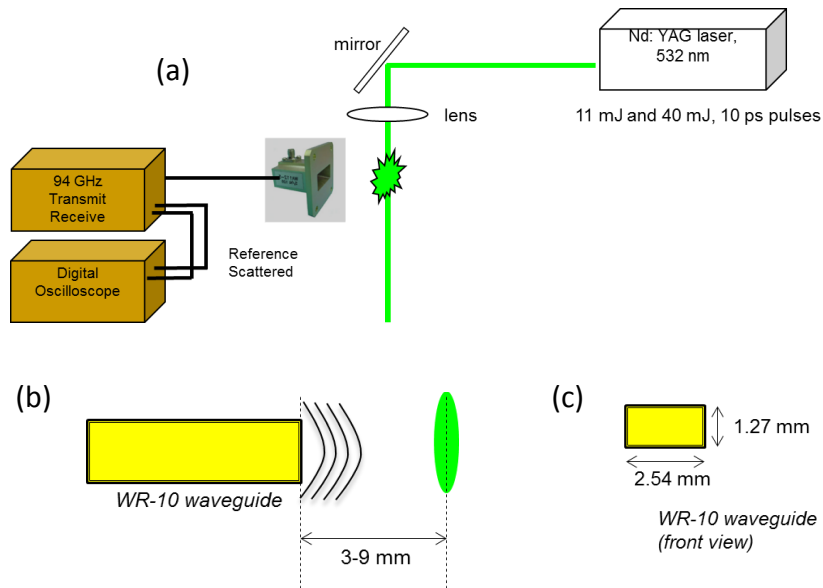


FIGURE 1. MI configuration for measuring ionized laser plume velocity. (a) shows the full system; (b) shows the ionization plume and waveguide relative positions, while (c) shows the cross sectional dimensions of the 94 GHz WR-10 waveguide

The finite element code HFSS¹⁴⁻¹⁶ was used to model the interaction of 94 GHz signal emerging from a rectangular WR-10 waveguide with a plasma plume. The plume was modeled as a perfect conducting solid. The radius of the ellipsoid was increased as a function of time to simulate the expanding plume. Different ellipsoid aspect ratios were simulated with an assumed expansion velocity of 880 m/s. The modeled configuration is shown in Figure 2. In the figure the long axis of the ellipsoid, parallel to the direction of laser propagation, is shown also to be parallel to the plane of the rectangular waveguide termination. The distance of center of the ellipsoid is 2.9 mm from the end of the waveguide.

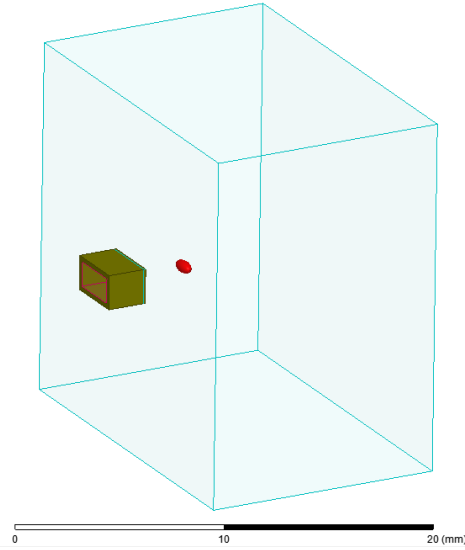


FIGURE 2. HFSS model geometry for finite element simulations of the plume/microwave interactions; the plume is 2.9 mm from the end of the WR-10 waveguide

RESULTS

A sequence of camera images of the ionization plume produced by a 10 ps laser pulse is shown in Figure 3, with inter-frame time 10 μ s. At 10 μ s after initiation the plume has an elliptical core and a spheroidal halo; the plume has expanded from a sub-mm focal spot such that the long axis of the elliptical core is about 5 mm long. The diameter of the spheroidal outer domain appears to be slightly smaller, around 4 mm. Note that we cannot exclude the possibility that the plume was briefly larger than imaged at a time earlier than 10 μ s, since the exposure time was 10 μ s. The plume intensity decays with time after 10 μ s so that by 30 μ s after initiation it is nearly undetectable with these camera settings.

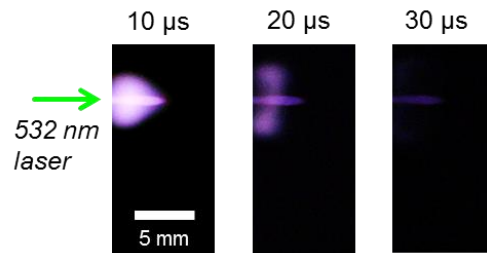


FIGURE 3. HFSS model geometry for finite element simulations of the plume/microwave interactions

HFSS model results of MI signal are shown in Figure 4. As indicated in Figure 2, the model assumes the long axis of the laser plume is parallel to the plane of the end of the waveguide. As the plume expands the measured power at the interferometer is calculated to pass through a minimum where the transmitted microwave signal destructively interferes with the reflected signal. Two different plume aspect ratios are simulated, 1:2 and 1:5, and the assumed velocity was 880 m/s. The plume was assumed to initiate 2.9 mm from the waveguide. Depending on the plume's velocity, aspect ratio, and initial position the reflected power minimum will be present at different times after initiation. For the 1:2 aspect ratio plume at 880 m/s, for example, the minimum is expected to appear at 0.8 microseconds after initiation, while for the 1:5 aspect ratio plume at 880 m/s the minimum should appear at 0.9 microseconds. This difference, while small, may be observable with 94 GHz MI, with further refinement of the technique.

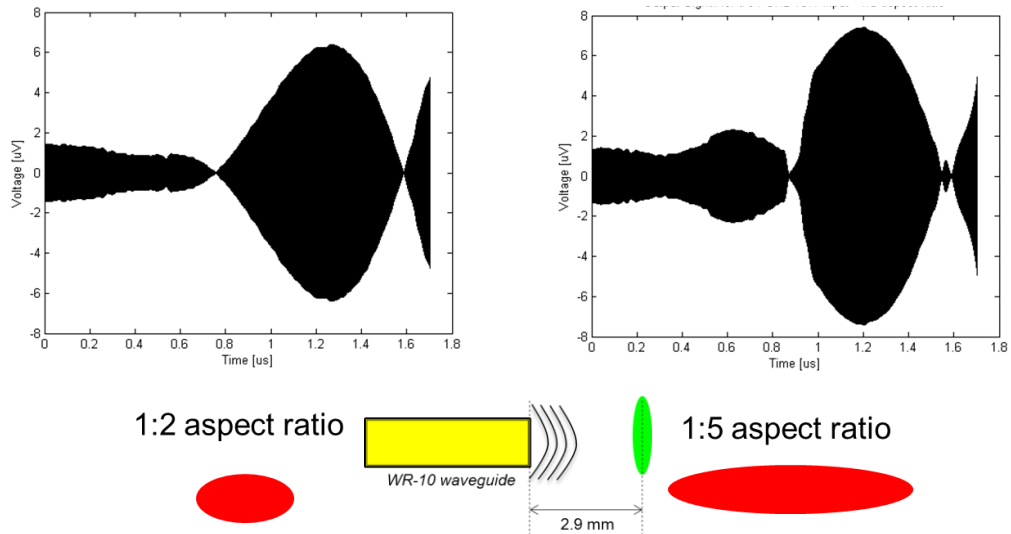


FIGURE 4. HFSS model geometry for finite element simulations of the plume/microwave interactions

The MI record is shown in Figure 5, for a plume created by a 10 mJ laser pulse at 9 mm, oriented now with the long axis of the plume perpendicular to the plane of the rectangular end of the waveguide. The minimum with the largest magnitude appears at about 2 microseconds after plume initiation. In an experimental configuration more directly comparable to the modeled figuration presented in Figure 4, the predicted minima were not observed.

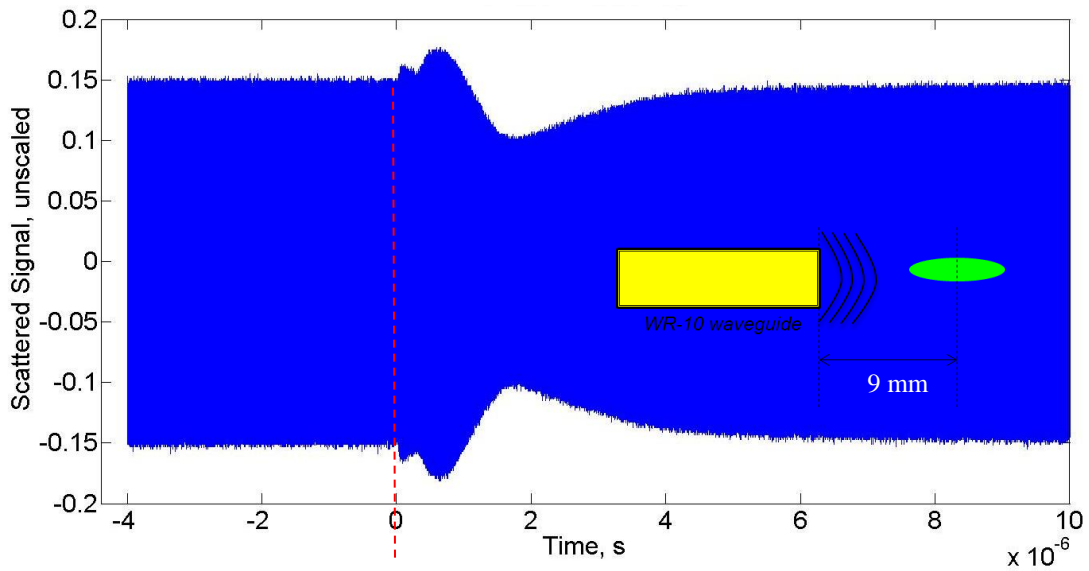


FIGURE 5. MI scattered power data from a 10 mJ laser pulse-initiated plume 9 mm from the end of the waveguide, with long axis perpendicular to the plane of the end of the waveguide. Time zero corresponds to the initiation time of the laser plume.

A typical MI record for a plume initiated 9 from the waveguide are shown in Figure 6. The plume was oriented with the long axis perpendicular to the plane of the rectangular end of the waveguide. There are two characteristic times associated with the measurement. Over the time labeled t_1 in Figure 6 ($0.2 \mu\text{s}$), the extracted phase velocity corresponds to a reflective front velocity of 1160 m/s. Over the time labeled t_2 in Figure 6 ($1.5 \mu\text{s}$), the average phase velocity corresponds to a reflective front velocity of about 325 m/s.

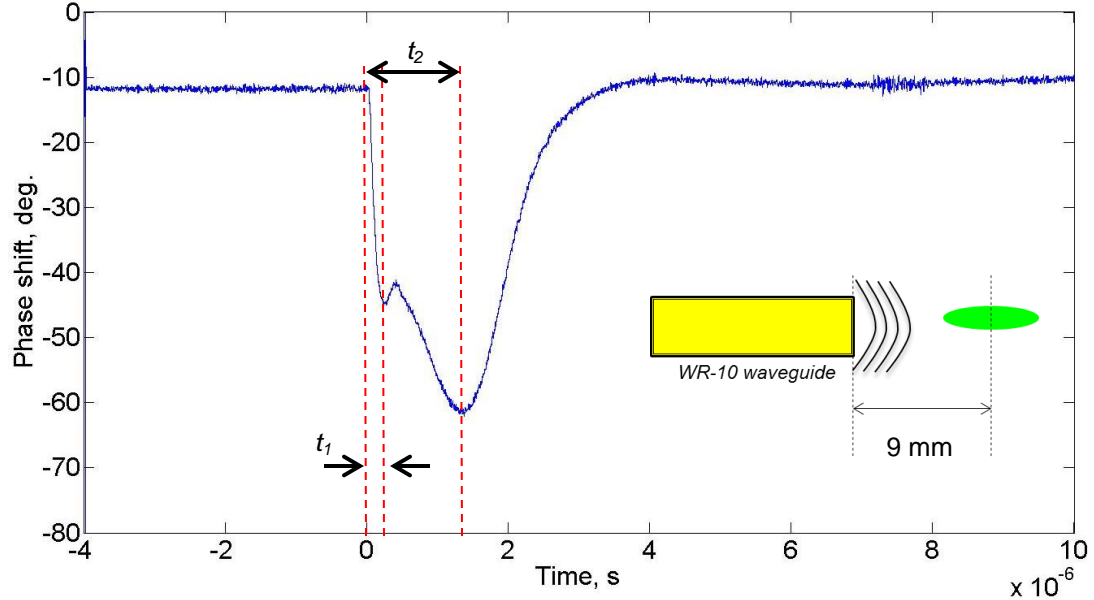


FIGURE 6. MI phase shift data from a 10 mJ laser pulse-initiated plume 9 mm from the end of the waveguide, with long axis perpendicular to the plane of the end of the waveguide. The reflective front velocity over t_1 corresponds to 1160 m/s, while the average reflective front velocity over t_2 corresponds to 325 m/s. Time 0 corresponds to the initiation time of the laser plume.

DISCUSSION

The HFSS model results in Figure 4 predict minima in the reflected power from an idealized plasma reflector modelled as a metallic conductor. However this model does not account for other sources of microwave absorption or reflection, such as the air shock which has been characterized by others.¹¹ Experimentally, we do not observe the predicted reflected power minima under conditions which are comparable to those modeled in terms of plume orientation and distance from the waveguide. We do observe more pronounced power fluctuations at a different laser power, and plume orientation and plume-waveguide separation, as demonstrated in Figure 5. The origin of these fluctuations is still under study, requiring more detailed coupling of optical images of the plume with the MI record. It is notable, however, that the beginning of power fluctuations is nearly coincident with the laser plume initiation time, time 0 in Figure 5. If the plumes we observe are comparable to those produced by others at smaller wavelengths,¹¹ then our observation implies that features on the order of a mm may be characterized by MI at 94 GHz.

In Figure 6 the front transit distance over t_1 is $1160 \text{ m/s} \times 0.2 \times 10^{-6} \text{ s}$, or about 0.2 mm. The front transit distance over t_2 is $325 \text{ m/s} \times 1.3 \times 10^{-6} \text{ s}$, or about 0.1 mm. For comparison, the wavelength of 94 GHz in air is about 3.2 mm. The speed of sound in air at room temperature is about 340 m/s, so the second feature in this record may be associated with an air shock. The faster time associated with the reflective front is more than 10 times slower than the $\sim 14000 \text{ m/s}$ observed optically by Pandey and Thareja under excitation conditions which are relatively comparable to those used here: 8 ns, 150-210 mJ, 1064 nm.¹³ The energies employed by Pandey and Thareja were 4-20 times larger, and wavelengths were 2 times longer, however. Most importantly, however, the velocities measured by Pandey and Thareja were at very early times – the first 300 ns of plume expansion. In a separate study with shorter wavelengths, 193 nm, by Thiagarajan and Scharer, velocity of the ionization plume was explicitly measured as a function of the time of the plume expansion.¹¹ This study found that the plume velocity was a very strong function of expansion time, dropping from 10,000 m/s at 0.2 μs after initiation to 2000-3000 m/s at 2 μs after initiation. The study also showed that the plume diameter increased comparably as a function of time, reaching the 94 GHz wavelength 3 mm at about 0.5 μs after initiation. As with the reflected power from this same experiment (Figure 5), it is interesting to note that the microwave signal in Figure 6 begins less than 0.1 μs after

pulse initiation, as determined by the photodiode trigger signal. If the plume diameter increases at a rate comparable to that observed by Thiyagarajan and Scharer, this again implies that some reflection is occurring even at subwavelength plume dimensions.

SUMMARY AND CONCLUSIONS

We use microwave interferometry (MI) to interrogate laser-initiated plasma plumes, which expand to a few mm in diameter at times much less than 10 μ s. Modeling the system with the finite element code HFSS, using the simplifying assumption that the plasma acts as a metallic conductor, we predict minima in reflected power at certain times after plasma initiation. These times are dependent on the plasma shape, orientation, position and velocity. Experimentally we observe variations in reflected power, but these do not appear to correlate with reflections from a single conductive surface. Additional experiments are required to better understand the source of these modulations, and to correlate them with plasma properties that can be represented by a simplified model. Phase changes in the reflected signal appear to correlate with a moving conductive surface at velocities 1160 m/s and 325 m/s. The 1160 m/s likely corresponds to the average velocity of an ionization plume surface, as it is comparable in magnitude to optically-observed plasma velocities from laser pulses. The 325 m/s may correspond to a reflection from an air shock. Together these results demonstrate significant promise for MI to characterize more complex hot spot behavior in solid explosives.

ACKNOWLEDGEMENT

This work was performed under the auspices of the U.S. Department of Energy by Lawrence Livermore National Laboratory under Contract DE-AC52-07NA27344, Lawrence Livermore National Security, LLC.

REFERENCES

1. M. A. Cook, R. L. Doran and G. J. Morris, *Journal of Applied Physics* **26** (4), 426-428 (1955).
2. J. L. Farrands and G. F. Cawsey, *Nature* **177** (4497), 34-35 (1956).
3. G. F. Cawsey, J. L. Farrands and S. Thomas, *Proceedings of the Royal Society of London Series a-Mathematical and Physical Sciences* **248** (1255), 499-521 (1958).
4. B. C. Glancy, A. D. Krall and H. W. Sandusky, *Shock Waves in Condensed Matter 1987. Proceedings of the American Physical Society Topical Conference*, 711-714 (1988).
5. B. C. Glancy, H. W. Sandusky and A. D. Krall, *Journal of Applied Physics* **74** (10), 6328-6334 (1993).
6. A. D. Krall, B. C. Glancy and H. W. Sandusky, *Journal of Applied Physics* **74** (10), 6322-6327 (1993).
7. V. M. Bel'skii, A. L. Mikhailov, A. V. Rodionov and A. A. Sedov, *Combustion Explosion and Shock Waves* **47** (6), 639-650 (2011).
8. P. J. Rae, B. B. Glover, J. A. Gunderson and W. L. Perry, in *Shock Compression of Condensed Matter - 2011, Pts 1 and 2*, edited by M. L. Elert, W. T. Buttler, J. P. Borg, J. L. Jordan and T. J. Vogler (2012), Vol. 1426.
9. J. W. Tringe, R. J. Kane, K. T. Lorenz, E. V. Baluyot and K. S. Vandersall, presented at the Conference of the APS Topical Group on Shock Compression of Condensed Matter (APS-SCCM), Seattle, WA, 2013 (unpublished).
10. M. E. Daily, B. B. Glover, S. F. Son and L. J. Groven, *Propellants Explosives Pyrotechnics* **38** (6), 810-817 (2013).
11. M. Thiyagarajan and J. E. Scharer, *Ieee Transactions on Plasma Science* **36** (5), 2512-2521 (2008).
12. L. Xingwen, W. Wenfu, W. Jian, J. Shenli and Q. Aici, *Journal of Applied Physics* **113** (24), 243304 (243306 pp.)-243304 (243306 pp.) (2013).
13. P. K. Pandey and R. K. Thareja, *23rd National Symposium on Plasma Science and Technology (Plasma-2008)* **208** (2010).
14. J. W. Bandler, R. M. Biernacki and S. H. Chen, *Fully automated space mapping optimization of 3D structures*. (1996).
15. H. M. Jafari, M. J. Deen, S. Hranilovic and N. K. Nikolova, *Ieee Transactions on Antennas and Propagation* **55** (4), 1184-1188 (2007).
16. Ansys, (2015), Vol. 2015.